Numerical Analysis of Heat Transfer and Temperature Distribution in Direct Metal Laser Sintering Method

Farshid Rajabi Varedehsaraei, Arman Maroufi *
Department of Mechanical Engineering, Faculty of Industrial and Mechanical Engineering, Qazvin Branch, Islamic Azad University, Qazvin, Iran
E-mail: F.rajabi@iaubanz.ac.ir, Armanmaroufi@qiau.ac.ir
*Corresponding author

Cyrus Aghanajafi
Department of Mechanical Engineering
K.N.Toosi University of Technology, Tehran, Iran
E-mail: Aghanajafi@ikntu.ac.ir

Mohammad Mehdi Kasaei
Department of Mechanical Engineering, Faculty of Industrial and Mechanical Engineering, Qazvin Branch, Islamic Azad University, Qazvin, Iran
E-mail: Kasaei@qiau.ac.ir

Abstract: In this research, the thermal analysis of additive fabrication by DMLS method has been investigated. In the DMLS method, the metal powder is melted by a laser heat source and finally a solid three-dimensional piece is formed. This analysis was performed by finite element method in Abaqus software. Laser heat distribution is considered Gaussian. The mechanical and thermal properties of the powder are considered as a function of melting temperature. Finally, the results obtained by the finite element method are compared with previous researches. The effects of laser speed and power on temperature distribution have also been investigated.

Keywords: DMLS, 3D Printing of Metals, Heat, Laser, Selective Laser Sintering

Biographical notes: Farshid Rajabi Varedehsaraei received his MSc in Mechanical Engineering, Energy systems from K.N.Toosi University of Technology in 2005. He is currently studying PhD in Mechanical Engineering at Azad University, Qazvin, and lecturer at the Department of Mechanical Engineering, Azad University, Anzali, Iran. His current research focuses on Rapid prototyping by 3D printer, thermodynamics and heat transfer. **Arman Maroufi** has MSc in Mechanical Engineering, Fluid mechanics and received his PhD in Mechanical Engineering from K. N. Toosi University in 2013. He is currently Assistant Professor at Qazvin Islamic Azad University. His current research focuses on thermodynamics and heat transfer. **Cyrus Aghanajafi** received his MSc in Mechanical Engineering from South Georgia State College and PhD and Postdoc in Mechanical Engineering from Tennessee State University in 1989. He is currently Professor at K.N.Toosi University. His current research focuses on thermodynamics and heat transfer. **Mohammad Mehdi Kasaei** received his PhD in Mechanical/ Manufacturing Engineering from Tarbiat Modares University in 2015. He is currently Assistant Professor at Qazvin Islamic Azad University. His research interests include metal forming, advanced manufacturing processes and mechanical behavior of materials.

1   INTRODUCTION

Making additives or what is commonly referred to as making by 3D printers, is a kind of production method in which the production of the piece is a completed layer by layer and the final shape of the piece is made. The main difference between different methods of making additives is the type of materials used, how the layers are made and how they are connected to each other [1]. Many experts refer to additive manufacturing technology as the Third Industrial Revolution and the future of research on this technology is such that even some industrialists believe that with significant advances in the field of additive manufacturing, manufacturing in the way it is done today will no longer exist and making in this way creates a new style in design and production [2-3]. In recent years, many improvements have been made in the development of materials, processes and machinery that enabled additive manufacturing processes to progress from prototype to rapid product prototype and transform industries such as aerospace and medical instruments.

Recently, many studies have been conducted to study temperature phenomena during the laser sintering process. Tang el al. [4] studied the thermal behavior and the effects of different process parameters on the quality and accuracy of a three-dimensional solid structure which is made of a special alloy based on copper. Simchi [5] has analyzed the effect of processing parameters on metal powder density in the direct metal laser sintering process. He made a connection between the density of metal powders and the laser energy during direct metal laser sintering, which was very useful for metals and alloys. Dong et al. [6] have proposed a transient three-dimensional finite element model. To simulate phase change during the laser sintering process by considering thermal and sintering phenomena, Zeng el al [7] developed a comprehensive thermal model for the selective laser fusion process using the Fourier thermal conductivity equation to investigate the temperature distribution in the powder layer. Jian el al [8] provides a three-dimensional transient model for temperature simulation in the laser powder selective process for aluminum coated with ceramic powder using a CO2 moving laser beam. Li and Gu [9] developed a finite element model to predict the relationship between processing parameters and thermal behavior when selecting AlSi10Mg powder using Ansys 12.0 software. The effect of laser power and laser scanning speed on thermal behavior and initial melt pool were analyzed and relevant experiments were also performed to study the microstructure of the structure under different conditions of the laser process to evaluate the physical reliability of the model. Yuan and Gu [10] developed a numerical model for the selective laser fluid of TiC/AlSi10Mg nanocomposites using the finite volume method and investigated the effect of process parameters on temperature distribution. A three-dimensional finite element model was proposed by Shi et al. [11] to investigate the effects of laser power and scanning speed on thermal behavior and melting mechanism for TiC/Inconel 71 powder. In this study, in order to optimize processing parameters, they discussed the mechanisms that make up processing defects such as impact, pores, clustering, and so on. Hu et al. [12] developed a finite element model for selective multilayer laser melting of AlSi10Mg powder. Parametric analysis was performed under different laser energy inputs. The effect of laser energy input on temperature field, melt pool depth, cooling rate and solidification morphology parameter was also investigated. The simulation results provide valuable theoretical guidance for the selection of laser particles of the AlSi10Mg molecule. Kundakcioglu et al. [13] investigated transient thermal analysis for the additive manufacturing of complex three-dimensional free-state structures in powder sintering systems and laser heat sources. A new particle-based discrete element model was proposed by Lee et al. [14] to investigate the effects of laser power, laser scanning speed and gate distance on the temperature distribution in the powder bed in the direct metal laser sintering process.

According to previous studies, in the present study, the mechanical and thermal properties of metal powder variable with melting temperature and heat distribution in the powder bed are considered in three dimensions.

2   METHODOLOGY

The aim of this project is numerical simulation of the DMLS process for a specific alloy, which will be a numerical method based on finite elements. The relationship between all the effective parameters proposed on the mechanical behaviour of the manufactured part will be investigated and compared with the results of resistance and mechanical tests and the optimal points will be determined. Three-dimensional simulation will also be performed in the Abaqus software. The heat distribution of the laser beam is assumed to be Gaussian. In addition, the powder particle shape is assumed to be spherical and the powder bed is considered to be continuous.

2.1. Powder Bed Modelling

To model the powder bed, according to previous studies, the optimal diameter and porosity of the powder should be selected. Ning et al. [15] by examining and comparing the powders with different diameters by mathematical and experimental methods, determined the diameter of 20 microns as the optimal diameter. They also found that the porosity can be considered equal to 0.1648. Therefore, in this study, the diameter of each

powder particle is considered to be 20 microns and the porosity is 0.1648.

2.2. Solving Governing Equations

In this section, first the governing equations are expressed and then numerical simulation is performed by finite element method in Abaqus software. Given that the heat source in the DMLS process is a laser, according to the thermal equilibrium relation, heat changes can be expressed based on the input energy obtained from a moving heat source as follows:

$$\frac{\partial \rho u}{\partial t} + \frac{\partial \rho HV}{\partial x} = \nabla.(k\Delta T) + \dot{q} \tag{1}$$

Where, u is the internal energy, H is enthalpy, ρ presents density, k shows thermal conductivity, $\dot{q}$ is heat source, t is time, x presents distance from the heat source, V is the velocity of the moving heat source in the direction of x and T is the temperature. Heat transfer equation by applying the following assumptions:

$$V = 0 \text{ , } du = cdT \text{ , } c\frac{\partial \rho T}{\partial t} = \nabla.(k\nabla T) + \dot{q}$$

It is obtained as follows:

$$\frac{\partial^2 T}{\partial x^2} + \frac{\partial^2 T}{\partial y^2} + \frac{\partial^2 T}{\partial z^2} = \frac{1}{\kappa}\frac{\partial T}{\partial} + \dot{q} \tag{2}$$

That:

$$\kappa = \frac{k}{\rho c}$$

Which, k, ρ and c are the coefficient of thermal conductivity, density and specific heat, respectively. The transient solution of the laser mobile heat source temperature according to the Gaussian heat distribution is as follows [16]:

$$\theta_{laser}(x,y,z,t) = \frac{P\eta}{8\rho c(\pi k)^{\frac{3}{2}}}\int_0^{t'}\frac{\exp\left[-\frac{(x-V(t-t'))^2 + y^2 + z^2}{4\kappa(t-t')}\right]}{(t-t')^{\frac{3}{2}}}dt' \tag{3}$$

Where, P is the power of the heat source, η is the heat absorption coefficient, t is the current time and t' is the previous time. To calculate heat loss by displacement and radiation, the following equations are written:

$$Q_{conv} = Ah(T-T_0) \tag{4}$$

$$Q_{rad} = A\varepsilon\sigma(T^4 - T_0^4) \tag{5}$$

Which, Q_{conv} and Q_{rad} are the heat loss due to displacement and radiation, A is the area of the heatsink, h is the displacement coefficient, ε shows emission, σ is the Stephen-Boltzmann constant, T is the temperature of the heatsink obtained by solving the heat transfer equation of the heat source and T_0 is the room temperature. Equivalent power for heat loss can be expressed as follows:

$$P_{equiv} = Ah(T-T_0) + A\varepsilon\sigma(T^4 - T_0^4) \tag{6}$$

The solution of the heatsink is also obtained as follows:

$$\theta_{\sin k}(x,y,z) = \frac{A}{4\pi\kappa R(T_m - T_0)}[h(T-T_0) + \varepsilon\sigma(T^4 - T_0^4)] \tag{7}$$

The density of the powder bed is calculated as follows:

$$\rho_p = (1-\varepsilon)\rho_s + \varepsilon\rho_g \tag{8}$$

Which, ρ_p is the density of the powder bed, ρ_s is the density of the solid part, ρ_g is the density of the air and ε is the volume fraction [16-17].

$$k_p = \frac{k_s(1-\varepsilon)}{1 + \psi\frac{k_s}{k_g}} \tag{9}$$

$$\psi = 0.02 \times 10^{2(\varepsilon - 0.3)} \tag{10}$$

Where, κ_p is the thermal conductivity of the powder bed, k_g is the solid thermal conductivity, ψ is the thermal conductivity of the air, the exponential factor and ε is the volume fraction of the empty space.

2.3. Finite Element Simulation

This section simulates the finite elements of the DMLS process. For laser thermal simulation, Abaqus software is linked to Fortran and all the equations of laser motion are written in Fortran. Another Fortran subroutine has also been used and coded to simulate changes in the properties of the powder bed.

To simulate the laser, to determine the appropriate Gaussian distribution of the laser beam, the DFLUX subroutine was used to implement the laser heat source with the Fortran code ("Fig. 1").

Laser Beam
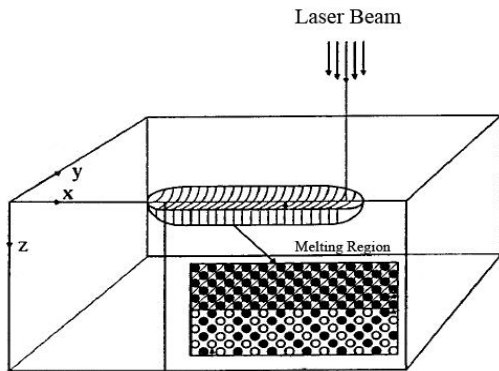
Fig. 1   Coordinates and schematic of laser motion.

The laser heat distribution equation is entered into Abaqus as the heat load. The following equation shows the Gaussian laser heat distribution:

$$q(r) = \frac{2P}{\pi r_0^2} e^{\frac{-2r^2}{r_0^2}} \qquad (11)$$

The above equation shows the thermal distribution relative to the center of the laser beam, where r is the distance from the laser radiation center, r_0 is the laser radius, P is the laser power, and q is the heat flux. The element used for the piece is considered solid and homogeneous. The meshing of the piece is done as "Fig. 2".
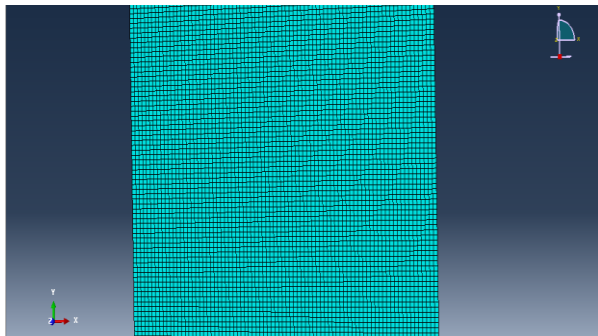
Fig. 2   mesh of powder bed.

The element type is considered C3D8T. To define the properties of the material, due to the powderiness of the alloy, the properties of the alloy are written by the subroutine UMAT.

3   NUMERICAL RESULTS AND DISCUSSIONS

In this section, the results of numerical solution are reviewed. First, the solution is validated with previous works, and the effects of laser speed and power on temperature distribution were then studied.

3.1. Numerical Solution Validation

First, in order to verify the heat distribution obtained, it is compared with the research of Dong et al. [18], which has been done numerically and experimentally. Dong et al. [18] examined a rectangle measuring $2 \times 1 \times 0.5$ mm made of titanium metal.

The initial temperature of the piece was considered to be 1800 Kelvin. Also, for modelling the powder bed, the density property of the material was considered as variable. Figure 3 shows that the present study is in good agreement with the research of Dang et al.
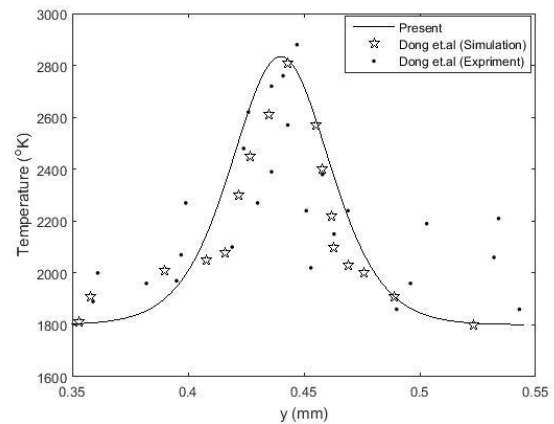
Fig. 3   Comparison of the present solution with the research of Dong et al [18].

Figure 4 shows the temperature diagram in terms of location for different powers. This diagram shows that increasing the power causes the temperature at the center point of the laser to increase. The considered dimensions are $8 \times 8 \times 0.2$ mm.
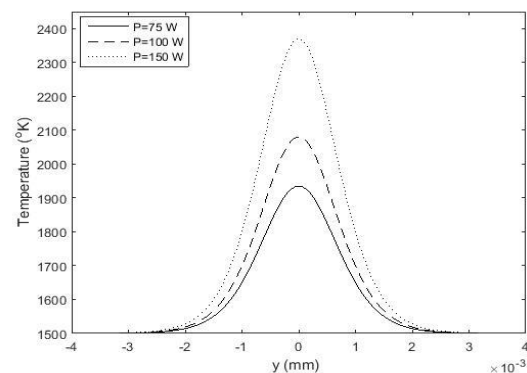
Fig. 4   Temperature distribution diagram in x direction for different powers.

Figure 5 shows the temperature changes for different scan speeds. Figure 5 shows that increasing the scan speed reduces the temperature penetration in the substrates. In fact, increasing the speed causes the underlying layers to have a lower temperature.
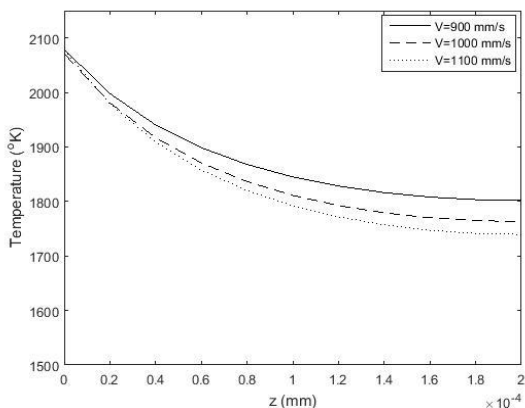
Fig. 5　Diagram of temperature distribution in z direction for different scan speeds.

Figure 6 shows a comparison of temperature and stress distributions for different initial temperatures (preheat). Table 1 shows the properties of Ti6Al4V alloy [19].

(a)

(b)

(c)
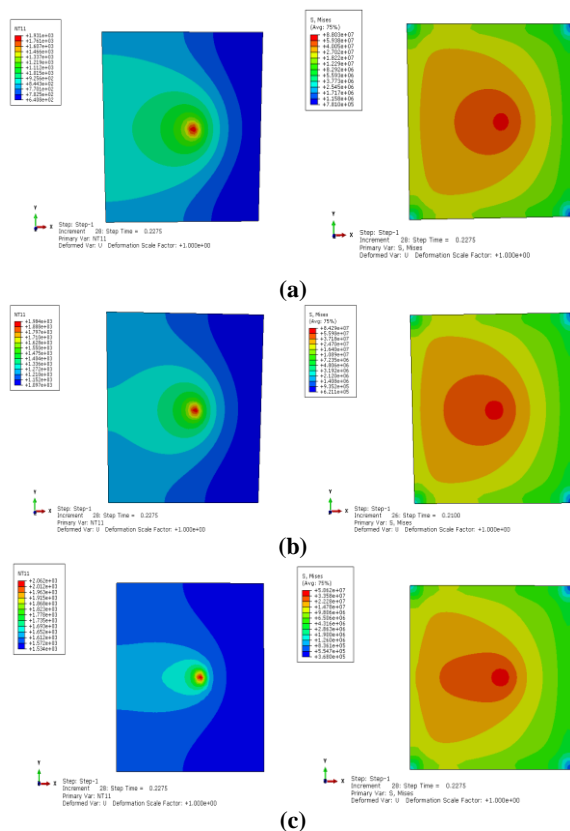
Fig. 6　Comparison of thermal stress and temperature for different initial temperatures: (a): 500, (b): 1000, and (c): 1500 (K).

As shown in "Fig. 6", the thermal stress decreases as the preheating temperature approaches the melting temperature. Also, the temperature and stress contour in the preheated temperature is 1500 K, the maximum

stress and temperature range is smaller than other temperatures.

Table 1 Properties of Ti6Al4V alloy [19]

Properties	Value	Symbol
Density kg / m^3	$(T < 2000)$　$(1-\tau)^\gamma \rho$ $(T > 2000)$　4428	ρ
Thermal conductivity of powder at temperature T_0 $W / (m.K)$	6.6	K_p
Thermal conductivity in solid state $W / (m.K)$	$(T < 2000) - 0.797$ $+18.2\times10^{-3}T - 2\times10^{-6}T^2$ $33.4\ (T > 2000)$	K_s
Specific heat capacity of powder at temperature T_0 $J / (kg.K)$	580	C_p
Solid state specific heat capacity $J / (kg.K)$	$(T < 2000)411.5$ $+2\times10^{-1}T - 5\times10^{-7}T^2$ $830\ (T > 2000)$	C_s
Latent heat J / kg	365000	H_f
Room temperature $^\circ K$	300	T_0
Solidus temperature $^\circ K$	1978	T_s
Liquidus temperature $^\circ K$	2003	T_l
Heat transfer coefficient $W / (m^2.K)$	24	h
Emission	0.9	ε
Stephen − Boltzmann constant $W / (m^2.K^4)$	5.67×10^{-8}	σ
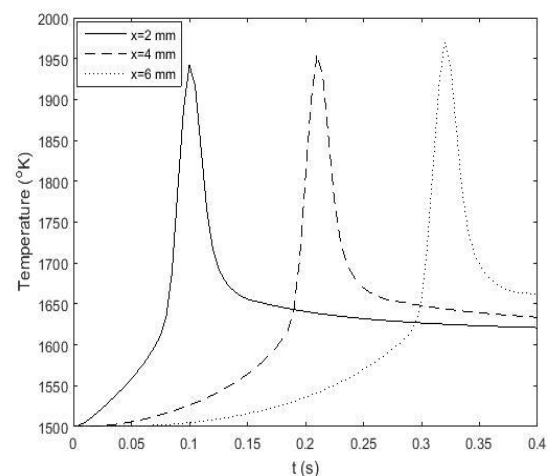
Fig. 7　Diagram of temperature change over time in different places.

Figures 7 and 8 show that with the laser movement, the temperature and stress of the elements increase compared to the temperature and stress of the previous elements.
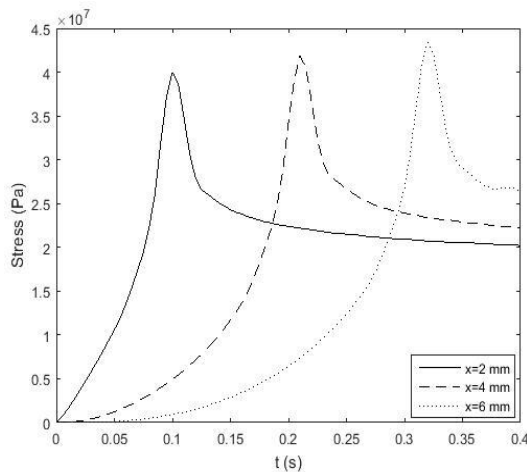
Fig. 8   Diagram of temperature change over time in different places.

4   CONCLUSION

In this research, a three-dimensional analysis of the additive production process by DMLS method has been performed. The solution method was performed using the finite element method in Abaqus software.

The research has yielded the following results:

- By approaching the preheating temperature to the melting point of the alloy, the thermal stress is reduced.
- As the laser scan speed increases, the temperature penetration in the underlying layers decreases and as a result, the underlying layer temperature decreases.
- The temperature of the elements is higher than the temperature of the previous element over time.

REFERENCES

[1]   Herzog, D., Seyda, V., Wycisk, E., and Emmelmann, C., Additive Manufacturing of Metals, Journal of Acta Materialia, Vol. 117, No. 15, 2016, pp. 371-92.

[2]   Simchi, A., Petzoldt, F., and Pohl, H., On the Development of Direct Metal Laser Sintering for Rapid Tooling, Journal of Materials Processing Technology, Vol. 141, No. 3, 2003, pp. 319-28.

[3]   Karapatis, N. P., Van Griethuysen, J. P. S., and Glardon, R, Direct Rapid Tooling: A Review of Current Research, Journal of Rapid prototyping, Vol. 4, No. 2, 1998, pp. 77-89.

[4]   Tang, Y., Loh, H. T., Wong, Y. S., Fuh, J. Y. H., Lu, L., and Wang, X., Direct Laser Sintering of a Copper-Based Alloy for Creating Three-Dimensional Metal Parts, Journal of Materials Processing Technology, Vol. 140, No. 1-3, 2003, pp. 368-72.

[5]   Simchi, A., Direct Laser Sintering of Metal Powders: Mechanism, Journal of Kinetics and Microstructural Features, Materials Science and Engineering, Vol. 428, No. 1-2, 2006, pp. 148-58.

[6]   Dong, L., Makradi, A., Ahzi, S., and Remond, Y., Three-Dimensional Transient Finite Element Analysis of the Selective Laser Sintering Process, Journal of Materials Processing Technology, Vol. 209, No. 2, 2009, pp. 700-6.

[7]   Zeng, K., Deepankar, P., and Stucker, B., A Review of Thermal Analysis Methods in Laser Sintering and Selective Laser Melting, Journal of in Proceedings of Solid Freeform Fabrication Symposium Austin, TX, Vol. 60, No. 1, 2012, pp. 796-814.

[8]   Jian, X., Weimin, S., and Rana, S. R., 3D Modeling and Testing of Transient Temperature in Selective Laser Sintering (SLS) Process, Journal of Optik, Vol. 124, No. 4, 2013, pp. 301–4.

[9]   Li, Y., Dongdong, G., Parametric Analysis of Thermal Behavior During Selective Laser Melting Additive Manufacturing of Aluminum Alloy Powder, Journal of Materials & Design, Vol. 63, No.1, 2014, pp. 856-67.

[10]   Yuan, P., Gu, D., Molten Pool Behaviour and Its Physical Mechanism During Selective Laser Melting of TiC/AlSi10Mg Nanocomposites: Simulation and Experiments, Journal of Physics D: Applied Physics, Vol. 48, No. 3, 2015, pp. 1–16.

[11]   Shi, Q., Gu, D., Xia, M., Cao, S., and Rong, T., Effects of Laser Processing Parameters On Thermal Behavior and Melting/Solidification Mechanism During Selective Laser Melting of TiC/Inconel 718 composites, Journal of Optics & Laser Technology, Vol. 84, No. 1, 2016, pp. 9–22.

[12]   Hu, H., Ding, X., and Wang, L., Numerical Analysis of Heat Transfer During Multi-Layer Selective Laser Melting of AlSi10Mg, Journal of Optik, Vol. 127, No. 20, 2016, pp. 8883–91.

[13]   Kundakcioglu, E., Lazoglu, I., and Rawal, S., Transient Thermal Modeling of Laser-Based Additive Manufacturing for 3D Freeform Structures, Journal of Advanced Manufacturing Technology, Vol. 85, No. 20, 2016, pp. 493–501.

[14]   Lee, W. H., Zhang, Y., and Zhang, J., Discrete Element Modeling of Powder Flow and Laser Heating in Direct Metal Laser Sintering Process, Journal of Powder Technology, Vol. 315, No. 1, 2017, pp. 300–08.

[15]   Ning, J., Wang, W., Ning, X., Sievers, D. E., Garmestani, H., and Liang, S. Y., Analytical Thermal Modeling of Powder Bed Metal Additive Manufacturing Considering

Powder Size Variation and Packing, Journal of Materials Vol. 13, No. 8, 2020, pp. 1988.

[16] Ning, J., Sievers, D. E., Garmestani, H., and Liang, S. Y., Analytical Modeling of In-Process Temperature in Powder Bed Additive Manufacturing Considering Laser Power Absorption, Latent Heat, Scanning Strategy, And Powder Packing, Journal of Materials, Vol. 12, No. 5, 2019, pp. 808.

[17] Criales, L. E., Arısoy, Y. M., and Özel, T., Sensitivity Analysis of Material and Process Parameters in Finite Element Modeling of Selective Laser Melting of Inconel 625, Journal of Advanced Manufacturing Technology, Vol. 86, No. 9-12, 2016, pp. 2653-66.

[18] Dong, L., Correia, J. P. M., Barth, N., and Ahzi. S., Finite Element Simulations of Temperature Distribution and of Densification of a Titanium Powder During Metal Laser Sintering, Journal of Additive Manufacturing, Vol. 13, No. 1, 2017, pp. 37-48.

[19] Ning, J., Sievers, D. E., Garmestani, H., and Liang, S. Y., Analytical Thermal Modeling of Metal Additive Manufacturing by Heat Sink Solution, Journal of Materials, Vol. 12, No. 16, 2019, pp. 2568.